Mg II h + k emission lines as stellar activity indicators of main sequence F-K stars

Andrea P. Buccino and Pablo J. D. Mauas

Instituto de Astronomía y Física del Espacio (CONICET), C.C. 67 Sucursal 28, 1428-Buenos Aires Argentina

Accepeted: March 27th, 2008.

ABSTRACT

Context. The largest dataset of stellar activity measurements available at present is the one obtained at the Mount Wilson Observatory, where high-precision Ca II H+K fluxes have been measured from 1966 for about 2200 stars. Since the Mg II h and k lines at λ2800 Å are formed in a similar way to the Ca II H+K emission lines, they are also good indicators of chromospheric structure. The *International Ultraviolet Explorer (IUE)* provides a large database of UV spectra in the band 1150-3350 Å, from 1978 to 1995, which can also be used to study stellar activity.

Aims. The main purpose of this study is to use the IUE spectra in the analysis of magnetic activity of main sequence F-K stars. Combining IUE observations of Mg II and optical spectroscopy of Ca II, the registry of activity of stars can be extended in time.

Methods. We retrieved all the high-resolution spectra of F, G, and K main sequence stars observed by IUE (i.e. 1623 spectra of 259 F to K dwarf stars). We obtained the continuum surface flux near the Mg II h+k lines near λ2800 Å and the Mg II line-core surface flux from the IUE spectra.

Results. We obtained a relation between the mean continuum flux near the Mg II lines with the colour $B-V$ of the star. For a set of 117 nearly simultaneous observations of Mg II and Ca II fluxes of 21 F5 to K3 main sequence stars, we obtained a colour dependent relation between the Mount Wilson Ca II S-index and the Mg II emission line-core flux. As an application of this calibration, we computed the Mount Wilson index for all the dF to dK stars which have high resolution IUE spectra. For some of the most frequently observed main sequence stars, we analysed the Mount Wilson index S from the IUE spectra, together with the ones derived from visible spectra. We confirm the cyclic chromospheric activity of ϵ Eri (HD 22049) and β Hydri (HD 2151), and we find a magnetic cycle in α Cen B (HD 128621)

Key words. Stars: activity of –Stars: late-type – UV radiation

1. Introduction

Stellar magnetic activity causes non-thermal heating of the outer atmospheres of cool stars. One of the principal diagnostics for solar and stellar chromospheric activity is the emission in the Ca II H and K resonance lines (at 3968 and 3934 Å). In particular, the largest dataset of activity measurements available at present, comprising observations of over two thousands stars, is the one obtained with the Mount Wilson HK spectrophotometers, which since 1966 measure high precision Ca II H+K fluxes. As an indicator of stellar activity, an index S has been defined as the ratio between the emission line-core flux and the flux in the continuum nearby.

Since the Mg II h and k lines (at 2803 and 2796 Å) are formed in a similar way to the Ca II H+K lines, they are also good indicators of the heating and the thermal structure of stellar atmospheres, especially from the high photosphere to the upper part of the chromospheric plateau. Furthermore, the Mg II resonance lines are more sensitive to weak chromospheric activity than the Ca II ones, because the adjacent near UV continuum is significantly weaker in the Mg II continuum and the photospheric line wings are darker at 2800 Å.

In the solar case, the Mg II core-to-wing ratio defined by Heath & Schlesinger (1986), has become a valuable index of variability of the chromospheric radiation. For the last twenty years, solar activity has been monitored from space by many instruments (SBUV, SOLSTICE, SUSIM and GOME). These observations have provided valuable data from which the Mg II index can be derived.

In order to connect stellar and solar observations, Cerruti-Sola et al. (1992) compared IUE Mg II profiles with some *Skylab* spectra of solar regions. They showed that different Mg II emission levels observed in stars of similar spectral type are due to differing fractions of their surfaces covered by magnetic regions.

In previous studies, it was found that the radiative fluxes of the Ca II and the Mg II lines are highly correlated among themselves (Oranje & Zwaan 1985, Schrijver 1987, and Rutten et al. 1991). Using nearly simultaneous observations, Schrijver et al. (1992) derived a linear relationship be-

Send offprint requests to: A. P. Buccino, e-mail: abuccino@iafe.uba.ar

tween the Mg II h+k fluxes ($F_{Mg\,II}$), measured using IUE[1] spectra, and the Mount Wilson Ca II H+K fluxes ($F_{Ca\,II}$).

The study of chromospheric variability requires at least a decade of data to reveal variations with timescales similar to the 11 yr solar cycle. IUE provides an extensive homogeneous database of UV spectra covering the band 1150-3350 Å, from 1978 to 1995. The purpose of this study is to intercalibrate the Mg II and Ca II observations, to combine IUE observations of Mg II h+k and visible observations of Ca II H+K and to extend in time the registry of activity of solar-type and cooler stars.

In Section §2, we first analyse the UV continuum adjacent to the Mg II lines. In Section §3, we derive a relation to determine the Mount Wilson index from the Mg II line-core flux. Finally, in Section §4 we study, for several main sequence stars, the Mount Wilson indices we obtained indirectly from IUE observation, the ones published by Henry et al. (1996) from CTIO spectra and the indices obtained from CASLEO spectra.

2. UV continuum near the Mg II lines

In Fig. 1 we present some examples of the high resolution IUE spectra of three F, G and K main sequence stars. The spectra are available from the IUE public library (at http://ines.laeff.esa.es/cgi-ines/IUEdbsMY), and have been calibrated using the NEWSIPS (New Spectral Image Processing System) algorithm (Garhart et al., 1997). The internal accuracy of the high resolution calibration is around 4% (Cassatella et al. 2000).

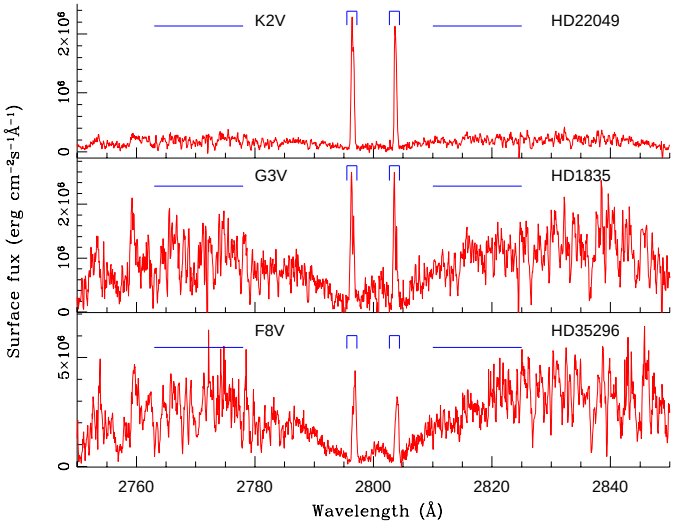

Fig. 1. IUE spectra of three representative stars: HD 22049 (K2V), HD 1835 (G3V) and HD 35296 (F8V). The windows used to integrate the continuum flux (2763-2778 Å and 2810-2825 Å) and the line-core emission (Mg II k: 2795.50-2797.20 Å and Mg II h: 2802.68-2804.38 Å) are marked.

The measured flux from the IUE spectra f was transformed to surface flux F using the Oranje et al. (1982) relation

$$log\,(F/f) = 0.35 + 0.4(m_V + BC) + 4\ log\,T_{eff}, \qquad (1)$$

[1] *International Ultraviolet Explorer*

where m_V is the visual apparent magnitude that we obtained from the *Hipparcos and Tycho Catalogue* (Perryman et al. 1997, Hoeg et al. 1997), BC is the bolometric correction obtained from Flower (1996) and T_{eff} is the effective temperature, from Boehm-Vitense (1981).

To analyse the UV continuum surface flux near the Mg II lines, we obtained all the high resolution spectra of F, G and K main sequence stars observed by IUE (i.e. 1623 spectra of 259 F to K dwarf stars), and we integrated the flux in two windows 15 Å wide centred at 2817.50 Å and 2770.50 Å ($F_{cont_{MgII}}$, Fig. 1). These windows are as wide as possible to obtain the best signal-to-noise relation, without including lines of chromospheric origin.

In Fig. 2, the log ($F_{cont_{MgII}}$) derived from each IUE spectrum is plotted against the colour $B-V$, from the Hipparcos and Tycho Catalogues. In our set of observations, the measured continuum flux presents a mean intrinsic variation of 30% for some stars; we will explore the source of this dispersion at the end of this section. For simplicity, we do not include the error bars in the figure. On the other hand, we neglect the errors in $B-V$ since they are very small.

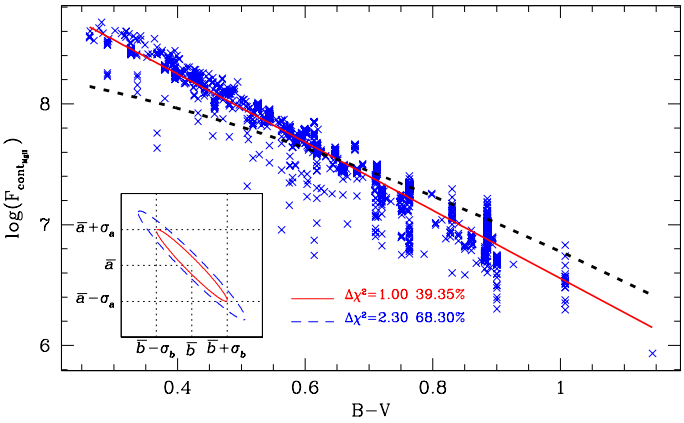

Fig. 2. log ($F_{cont_{MgII}}$) vs. $B-V$ for 1623 high resolution IUE spectra of 259 stars. The solid line shows the best linear interpolation and the dashed line is the relation obtained by Rutten (1984) for the visible continuum surface flux. In the inset, we show the χ^2 contours of the 39.3% (full line) and 68.3% (dotted line) confidence levels for the two fitted parameters, assuming that they present normal distributions with mean values and standard deviations: $\overline{a} = -2.823$, $\sigma_a = 0.018$ and $\overline{b} = 9.376$, $\sigma_b = 0.013$.

For the data plotted in Fig. 2, we found a good linear regression $\log(F_{contMgII}) = b(B-V) + a$, with a correlation coefficient R=0.97. The best fit is given by

$$\log(F_{contMgII}) = (-2.823\pm0.018)(B-V)+(9.376\pm0.013). \qquad (2)$$

Therefore, we obtain an exponential relation between an average UV continuum surface flux and the colour $B-V$. The mean value $\langle F_{cont_{MgII}}\rangle$ and the standard deviation $\sigma_{F_{cont_{MgII}}}$ are:

$$\langle F_{cont_{MgII}}\rangle = 2.38\times10^{9}\times10^{-2.82(B-V)}\,\mathrm{erg\,cm^{-2}\,s^{-1}}, \qquad (3)$$

$$\sigma^2_{F_{cont_{MgII}}} = \langle F_{cont_{MgII}}\rangle^2\, P_2(B-V), \qquad (4)$$

with $P_2(B-V) = [9.5 + 1.3(B-V) + 1.5(B-V)^2]\times10^{-3}$.

The regression in Eq. 3 is significant at nearly a 70% confidence level, which tests satisfactorily the linear fit in Fig. 2.

In contrast, Schrijver et al. (1989) assumed that the Mg II continuum surface flux has the same dependence on colour than the one obtained by Rutten (1984) for the Ca II continuum. Rutten found that the logarithm of the visible continuum surface flux was proportional to a third order polynomial on $B-V$. In Fig. 2 we represent this relation with a dashed curve. It can be seen that the linear relation we obtained fits the observations better.

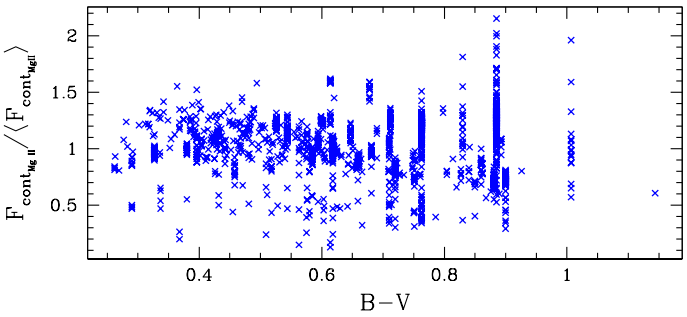

Fig. 3. The continuum surface flux $F_{cont_{MgII}}$ normalized to the averaged surface UV continuum $\langle F_{cont_{MgII}}\rangle$ vs. $B-V$ for the 1623 high resolution IUE observations.

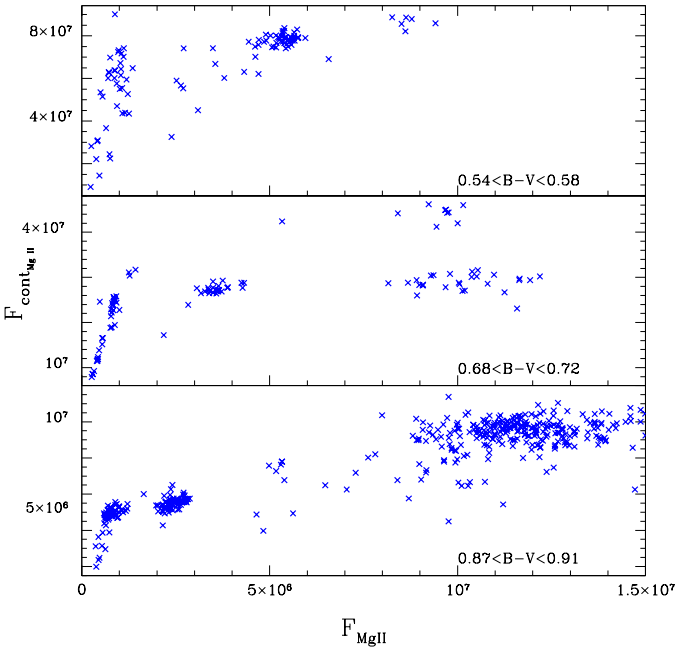

Fig. 4. $F_{cont_{MgII}}$ vs. F_{MgII}, for a set of main sequence stars with $0.54<B-V<0.58$ (*top*), $0.68<B-V<0.72$ (*middle*) and $0.87<B-V<0.91$ (*bottom*).

To analyse whether the spread in the data in Fig. 2 could be due to a remaining colour-dependent component in the continuum flux, we plot in Fig. 3 the ratio of the UV emission $F_{cont_{MgII}}$ to the value given by Eq. 3. The mean value of this ratio is 1.04 and the residuals present a flat distribution vs. $B-V$. We applied a Wilcoxon two-sample test (Frodesen et al., 1979) to the data plotted in Fig. 3 and we obtained that the fluctuations of the ratio $F_{cont_{MgII}}/\langle F_{cont_{MgII}}\rangle$ are within the statistical error with a confidence level of 90%. Therefore, we conclude that the spread in the data is not associated with a colour dependent component.

On the other hand, since the Mg II continuum is originated in the upper photosphere and the lower chromosphere of the star, it can be sensitive to activity. In fact, since the vertical spread for a specific colour $B-V$ in Fig. 3 corresponds, in most cases, to different observations of a single star, it is probably due to different levels of chromospheric activity.

To check this, in Fig. 4 we plot the continuum surface flux $F_{cont_{MgII}}$ vs. the Mg II line-core emission F_{MgII} for three different colour bins. To integrate the Mg II line-core fluxes, we found that the best integration window in the lines for high resolution IUE spectra are two 1.70 Å wide passbands centred at 2803.53 Å and 2796.35 Å (see Fig. 1). The position and the width of the integration windows were chosen to guarantee that the contribution of the integrated flux is merely chromospheric, beyond the basal contribution.

The Ca II continuum flux, used in the Mount Wilson index definition, is associated with photospheric emission and chromospheric activity is insignificant in this wavelength range. In contrast, in Fig. 4 we note that, independently from the colour, the $F_{cont_{MgII}}$ increases with the Mg II line-core flux and, therefore, the continuum flux depends to some extent on the activity level. For this reason, we did not attempt to build an activity index as the ratio in the fluxes in the Mg II line-cores and the continuum, similar to the S index.

3. Mg II h+k and Ca II H+K emission index calibration

To obtain the Mount Wilson index S indirectly from the UV spectra, we analysed the relation between the Ca II-index and the Mg II line-core flux. To guarantee that both diagnostics represent the same phase of activity of the star, we used 117 nearly simultaneous observations (i.e. with a time interval lower than 36 hours) of Ca II and Mg II line-core surface fluxes.

These observations of 21 stars with $0.45 \leq B-V \leq 1.00$ (see Table 1) are included in the dataset used by Schrijver et al. (1992) to intercalibrate Ca II and Mg II surface fluxes. We excluded from Schrijver's list HD 188512 due to its noisy IUE spectrum and some observations of HD 3651 where the ratio between the Mg II k to h line fluxes is greater than 1.55 (i.e. where the k/h ratio deviates in more than 2σ from the mean).

Rutten (1984) found a relation between the Ca II line-core surface flux and the Mount Wilson index S for main sequence stars with $0.30 \leq B-V \leq 1.60$

$$F_{CaII} = F_H + F_K = S\, C_{cf}\, T_{eff}^4\, 10^{-14}, \qquad (5)$$

where the conversion factor C_{cf} is given by

$$\log(C_{cf}) = 0.25(B-V)^3 - 1.33(B-V)^2 + 0.43(B-V) + 0.24,$$

and F_H and F_K are the Ca II H and K surface fluxes expressed in arbitrary units, which differ from an absolute calibrated scale by a multiplicative factor 1.29×10^6 erg cm^{-2} s^{-1}.

From the F_{CaII} values listed in Schrijver et al. (1992), we obtained the Mount Wilson S using Eq. 5. On the other

Table 1. Stars used in the Mg II - Ca II calibration.

Stars HD	Spectral Class and Type	m_v	$B-V$	T_{eff} (K)
1835	G3V	6.39	0.66	5675
9562	G0V	5.76	0.64	5750
10700	G8V	3.50	0.72	5500
17925	K0V	6.04	0.87	5170
20630	G5V	4.83	0.68	5610
22049	K2V	3.73	0.88	5140
26965	K1V	4.43	0.82	5295
35296	F8V	4.99	0.53	6185
39587	G0V	4.41	0.59	5950
45067	G0V	5.87	0.56	6060
101501	G8V	5.33	0.72	5500
114378	F5V	5.22	0.45	6540
115383	G0V	5.22	0.59	5950
115404	K3V	6.52	0.94	4990
131156	G8V	4.72	0.72	5500
141004	G0V	4.43	0.60	5910
143761	G2V	5.41	0.60	5910
149661	K0V	5.75	0.82	5295
152391	G8V	6.64	0.76	5295
154417	F8V	6.01	0.58	5985
187013	F5V	4.99	0.47	6445

hand, we measured the Mg II line-core flux F_{MgII} on the corresponding 117 high resolution IUE spectra. The results are shown in Fig. 5.

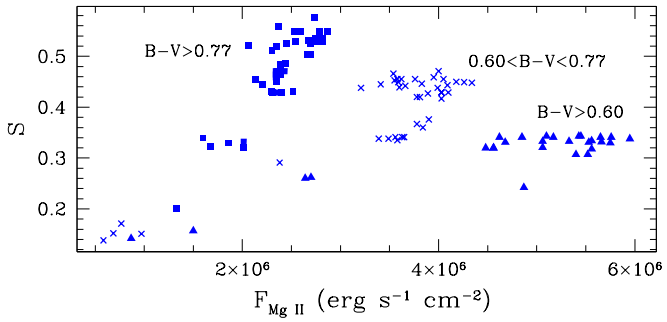

Fig. 5. S vs. F_{MgII} for three different colour bins: $B-V>0.77$ (squares), $0.60<B-V<0.77$ (crosses) and $B-V<0.60$ (triangles).

The main source of error in our data is the dispersion in F_{MgII}, due to the fact that there is a single value of F_{CaII} for IUE spectra differing in less than 36 hours. We found that the standard deviation of these F_{MgII} values could be up to 10%. Therefore, we used in the calibration an average of the F_{MgII} values which were assigned a single F_{CaII} and an error of 10% for F_{MgII}. Our dataset was consequently reduced to 93 points.

In Fig. 5 it can be seen that, as colour increases, the slope of the relation between the Mg II flux and the S index also increases. This could be due to different reasons: on one hand, the Mount Wilson index calculation involves the continuum flux near the Ca II lines, which of course depends on $B-V$. On the other hand, a colour dependent basal flux, independent from the activity level of the star, could also be present in the Mg II and the Ca II line-core emission. Many studies (e. g. Schrijver et al. 1989, Rutten et al. 1991) showed that the basal flux in the chromospheric lines decreases as $B-V$ increases and that the Mg II basal flux is lower than the Ca II one.

Therefore, a colour dependent S-F_{MgII} calibration is needed for these data. Here, we proposed an S-F_{MgII} calibration given by

$$S = a\,(B-V)^{\alpha}\,F_{MgII} + b\,, \tag{6}$$

whith F_{MgII} expressed in erg cm^{-2} s^{-1}, and we found that the best correlation coefficient (R=0.95) is obtained for α=(3.0 $\pm$ 0.1). Considering the errors in both coordinates and minimizing the expression

$$\chi^2 = \Sigma_{i=1}^{N} \frac{(y_i - b - a x_i)^2}{\sigma_{y_i}^2 + a^2\sigma_{x_i}^2}, \tag{7}$$

where $y \equiv S$ and $x \equiv F_{MgII}(B-V)^{\alpha}$, we obtained that the best parameters are $a = (2.310 \pm 0.052) \times 10^{-7}$ and $b = 0.109 \pm 0.004$, whith a reduced $\chi^2 = 1.07$ for an uncertainty of 6% in the S values. In Fig. 6 we plot the Mount Wilson index S and the Mg II line-core surface flux corrected in colour and the best linear fit given by Eq. 6.

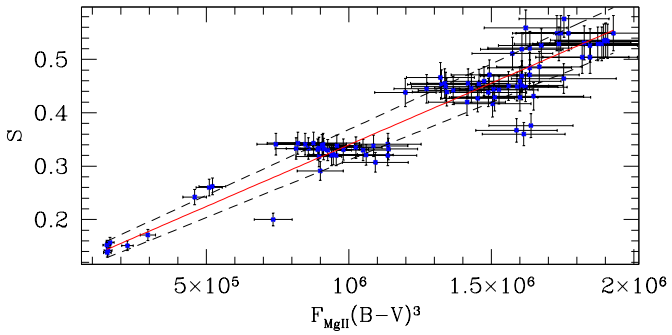

Fig. 6. S vs. $F_{MgII}(B-V)^3$ for the stars listed in Table 1. The errors are assumed to be 10% for F_{MgII} and 6% for S. The least square fit (solid line) has a correlation coefficient of 0.95. The dotted lines indicate $\pm 3\sigma$ from the fit.

4. Application of the calibration

As an application of the calibration obtained in Eq. 6, we have measured the Mg II line-core flux on all the 1623 IUE high resolution spectra available for main sequence stars of spectral types F to K, and then converted the surface flux F_{MgII} to the Mount Wilson index. These results are presented in Table 3.

For several of the most observed main sequence stars, we analysed the Mount Wilson index S inferred from the IUE spectra, together with the ones obtained from CTIO spectra (Henry et al., 1996) and from CASLEO spectra with the calibration of Cincunegui et al. (2007). In this way our observations cover the period between 1978 and 2005. Even if, for most stars, the density of measurements along the years is low, we can infer the level of activity and its variability for the whole period and during short intervals of time. For these stars, we list in Table 2 the average, maximum and minimum level of activity reached along decades (columns

4 and 5) and the variations recorded in particular years (column 6).

For those stars in Table 2 that were observed for decades and for which we have a large number of measurements, in what follows we plot the index S vs. time and we analyse their magnetic behaviour in detail.

HD 1835 - BE Ceti

As expected, the BY Dra stars (HD 1835 and HD 22049) show very strong chromospheric activity. In particular, HD 1835(G3V) is a young star only 600 Myr old, with a rotation period of 7.78 days (see references in Table 2). Baliunas et al. (1995), studying data for the period 1966-1991, reported that it presents an activity cycle with a length of 9.1 ± 0.3 years. In Fig. 7 we show our data for this star. Unfortunately, we are not able to check this period from these data, as they are insufficient to build a periodogram and obtain a significant result. However, we can infer that the level of activity slightly increased in the period 2000-2005 with respect to the previous years. From Fig. 7 we obtain that HD 1835 reached a maximum level of activity S_{max}=0.354, a minimum level S_{min}=0.244 and a mean level $\langle S \rangle$ =0.332 between 1978 and 1995, while between 2000 and 2004 these values were S_{max}=0.389, S_{min}=0.308 and $\langle S \rangle$ =0.347.

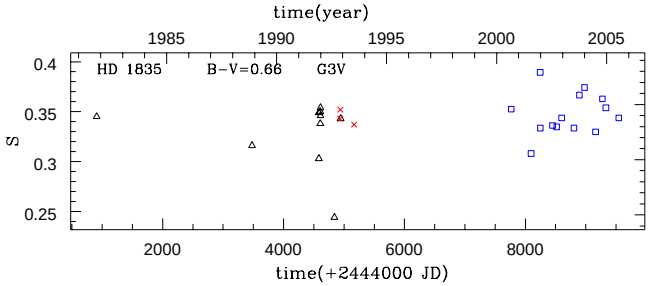

Fig. 7. Data for HD 1835. We indicate the Mount Wilson index S obtained from the IUE spectra with triangles (△), the one obtained by Henry et al. (1996) from CTIO spectra with crosses (×) and the one obtained from CASLEO spectra with square dots (□).

HD 22049 - ϵ Eri

HD 22049 (ϵ Eri, K2V) is a young and chromosperically active star ∼0.8 Gyr old with a rotation period of 11.28 days (see references in Table 2). Baliunas et al. (1995) reported that HD 22049 is a variable star without an evident cyclic behaviour, but Gray & Baliunas (1995) reported an underlying magnetic cycle with a period of the order of 5 years from 1986 to 1992. Hall et al. (2007) found that ϵ Eri is a high-activity variable star with a mean level of activity given by $\langle S \rangle = 0.516$ between 1994 and 2005. From our data, we obtained a $\langle S \rangle = 0.479$ for this time interval, which coincides with Hall et al.'s results within the statistical error.

In Fig. 8 we show our data for this star, where we observe appreciable short-scale (∼ months) variations from 10% to 25%.

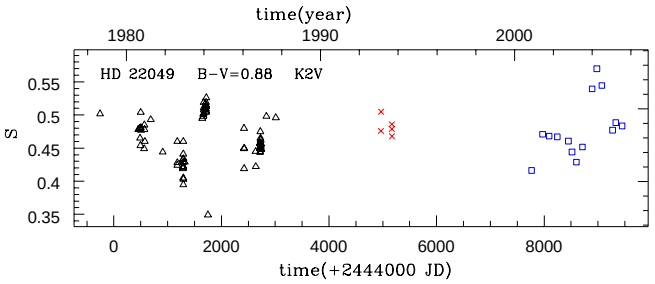

Fig. 8. Data for HD 22049. Symbols as in Fig. 7.

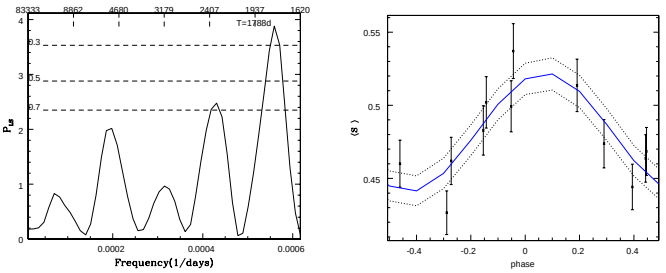

Fig. 9. HD 22049. *Left*: Lomb-Scargle periodogram of the mean annual $\langle S \rangle$ of the data plotted in Fig. 8. The False Alarm Probability (FAP) levels of 30, 50 and 70% are indicated. *Right*: The mean annual $\langle S \rangle$ of the data plotted in Fig. 8 phased with the period of 1788 days. The solid line shows the harmonic curve that best fits the data with a 60% confidence level and the dashed lines indicate the points that apart $\pm 3\sigma$ from that fit.

For our time interval (1978-2004), we analysed the mean annual $\langle S \rangle$ as a function of time with the Lomb-Scargle periodogram (Scargle 1982, Horne & Baliunas 1986), using the algorithm given by Press et al. (1992). This periodogram is shown in Fig. 9(a), where it can be seen that there is, indeed, a peak at 1788 days (∼4.9 years), with a false alarm probability (FAP) of 22%. In Fig. 9(b), we plot the mean anual $\langle S \rangle$ phased with the period obtained (1788 days) and we found that an harmonic function fits these points with a 60% confidence level.

HD 10700 - τ Ceti

HD 10700 (τ Ceti, G8V) is an old slow rotator (see Table 2), known to be rather constant in activity (Gray & Baliunas, 1994). In particular, Baliunas et al. (1995) analysed the Mount Wilson index from 1966 to 1991, and found that the chromospheric activity of this star is almost flat with a mean $\langle S \rangle = 0.171$. They proposed that it could be in a magnetic phase analogous to the solar Maunder minimum. They also found that HD 10700 is possibly increasing its level of activity since 1989.

Judge et al. (2004) compared solar UV spectra with several STIS spectra of HD 10700 from *Hubble Space Telescope* obtained in August, 2000, and concluded that its line spectrum may represent a solar spectrum corresponding to the Maunder minimum. On the other hand, they also found evidence of a weak magnetic field in HD 10700. Therefore, Judge et al. (2004) proposed that this star has temporally slipped into an extended magnetic quiescence (like the solar

Maunder minimum) and has only occasional active regions because of a small-scale turbulent dynamo.

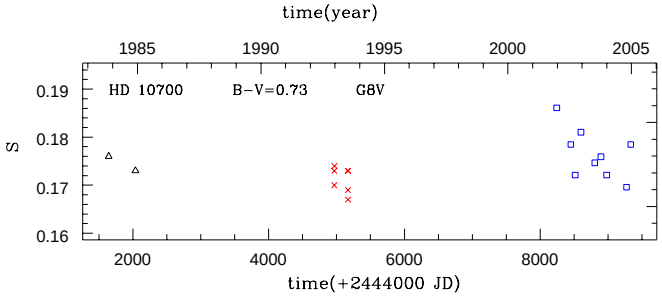

Fig. 10. Data for HD 10700. Symbols as in Fig. 7.

From the few data plotted in Fig. 10, we observe that the mean level of activity of HD 10700 seems to increase in 2001. In particular we obtained a mean $\langle S \rangle = 0.172 \pm 0.001$ between 1978 and 1995, in agreement with the value given by Baliunas et al. (1995), and $\langle S \rangle = 0.176 \pm 0.003$ between 2001 and 2005. We also note a ∼10% variation from maximum to minimum between the end of 2001 and 2002, which could be attributed to faint magnetic events.

In summary, we find that HD 10700 could have increased its level of activity since 2001, and that its chromospheric variability in the period 2001-2005 is also appreciable. Therefore, our results are in agreement with the model proposed by Judge et al. (2004) of an underlying turbulent dynamo responsible for the few signs of magnetic activity in this star.

HD 2151 - β Hyi

Dravins et al. (1993) affirm that HD 2151 (β Hyi, G2IV) can be considered an evolved Sun, with a well-determined age of ∼6.7 Gyr (Dravins et al., 1998), and a magnetic activity cycle probably longer than the solar one (15-18 years). In Fig. 11 we plot our data for this star. With these data, we obtain a mean chromospheric variation of 22% from 1978 to 1995. On the other hand, the short-scale variations registered in 1985, 1993 and 1994 do not exceed 17%.

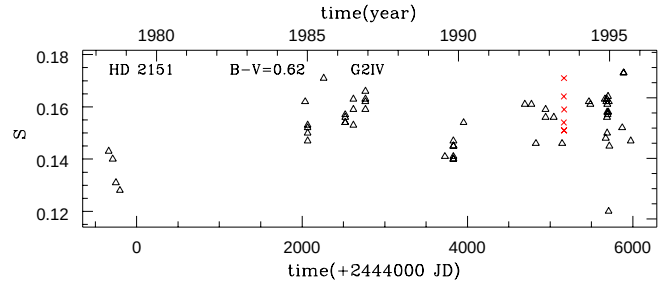

Fig. 11. Data for HD 2151 (β Hyi). Symbols as in Fig. 7.

To explore the magnetic behaviour of this star, we analysed the mean annual $\langle S \rangle$ with the Lomb-Scargle algorithm, and we obtained a cyclic behaviour with a period of 4117 days (∼11.28 years), with a FAP of 35%. The periodogram is plotted in Fig. 12(a). In Fig. 12(b) we show the mean annual $\langle S \rangle$ phased with this period and the harmonic curve

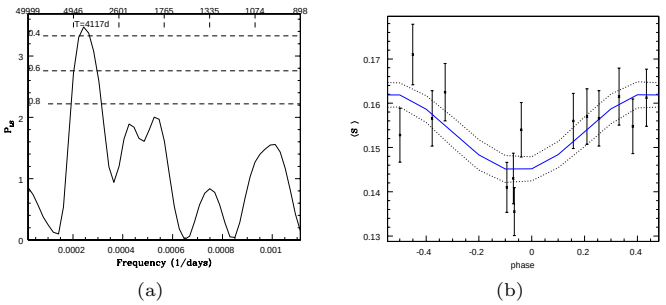

Fig. 12. HD 2151 (β Hyi). *Left*: Lomb-Scargle periodogram of the mean annual $\langle S \rangle$ in Fig. 11. The False Alarm Probability levels of 40 to 80% are indicated. *Right*: The mean annual $\langle S \rangle$ of the data plotted in Fig. 11 phased with the period of 4117 days. The solid line represents the harmonic curve that best fits the data with a 50% confidence level and the dashed lines indicate the points that appart $\pm 3\sigma$ from that fit.

that best fits the data with a good confidence level of 50%. Recently, Metcalfe et al. (2007) also obtained a ∼12 year-magnetic activity cycle for HD 2151 by analysing a Mg II index derived from the same IUE data plotted on Fig. 11 and they also found a faint correlation between this activity cycle and astereosismic observations.

HD 128620 - α Cen A

The non-interactive 79.2 yr binary system α Centauri is composed by the G2V star HD 128620 (α Cen A) and the K1V star HD 128621 (α Cen B), with a relative distance of 23.50 AU (Kamper & Wesselink, 1978). Both stars have different levels of activity. From 1978 to 2004, HD 128620 presented a mean annual index $\langle S \rangle$=0.167 while HD 128621 presented $\langle S \rangle$=0.214.

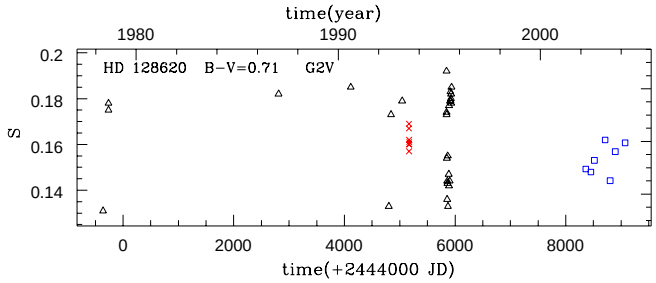

Fig. 13. Data for HD 128620. Symbols as in Fig. 7.

α Cen A is considered a good solar-twin (G2V, ∼ 1.09 $M_\odot$, solar abundances). In particular, Cerruti-Sola et al. (1992) reported that it has a UV spectrum similar to the inactive Sun, and Judge et al. (2004) concluded that HD 128620 provides a good proxy for the Sun's UV spectrum during an intermediate phase of the solar activity cycle. From our data, which is plotted in Fig. 13, we found that the mean annual $\langle S \rangle$ presented an 11% variation along 16 years (1978-2004), which is in agreement with the analogy of HD 128620 with a Sun of moderate activity. However, in Table 2 we observe an appreciable short-scale chromospheric variation (∼44%) in the index S during 1995, much larger than what is observed in the Sun. Therefore,

HD 128620 probably presents larger chromospheric features than the Sun.

Recently, Robrade et al. (2005) found that HD 128620 has decreased its X-ray flux by at least an order of magnitude during their observation program (from March 2003 to February 2005), and they attributed this variation to an irregular event or an unknown coronal activity cycle. To search for a magnetic cycle analogous to the solar one, we analysed the mean annual $\langle S \rangle$ of the data plotted in Fig. 13 with the Lomb-Scargle periodogram, but we did not find a periodic behaviour.

HD 128621 - α Cen B

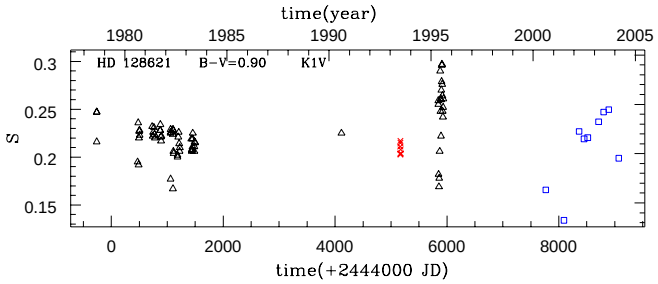

Fig. 14. Data for HD 128621. Symbols as in Fig. 7.

From ROSAT observations, Schmitt & Liefke (2004) reported HD 128621 as a flare star as it presented variations of nearly 30% in its X-ray emission during 20 days in August 1996. The data for this star are shown in Fig. 14, where it can be seen that, during 1995, it presented a chromospheric variation close to 75%, which could be attributed to a flare-like process. However, the light-curve for this event, which is shown in Fig. 15, does not present the typical characteristics of flares.

To study if this variation is due to rotational modulation, we analysed the data in Fig. 15 with the Lomb-Scargle periodogram and we obtained a period of 35.1 days, similar to the values that can be found in the literature for the rotation period. In particular, Saar & Osten (1997) estimated a rotation period of 42 days for HD 128621, while Jay et al. (1997) obtained a value of ∼37 days. Therefore, the variation found in Fig. 15 is probably due to rotation, for which we obtain a period of 35.1 days.

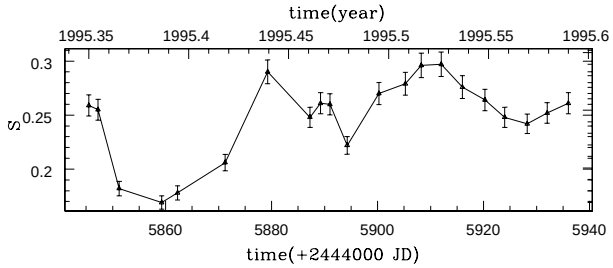

Fig. 15. Detail of Fig. 14 in 1995, showing a 35 day-modulation in the light-curve.

To analyse the magnetic behaviour of HD 128621, we studied the mean annual $\langle S \rangle$ of the data plotted in Fig. 14

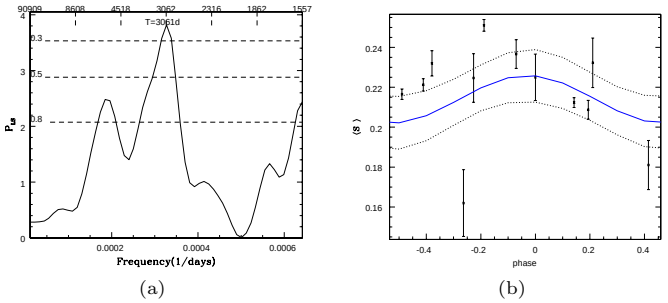

Fig. 16. HD 128621.*Left*: Lomb-Scargle periodogram of the mean annual $\langle S \rangle$ in Fig. 14. The False Alarm Probability levels of 30, 50 and 80% are indicated. *Right*: The mean annual $\langle S \rangle$ of the data plotted in Fig. 14 phased with the period of 3061 days. The solid line represents the harmonic curve that best fits the data with an 80% confident level and the dashed lines indicate the points that apart $\pm 3\sigma$ from that fit.

with the Lomb-Scargle periodogram, shown in Fig. 16(a). We obtained a magnetic cycle with a period of 3061 days (∼ 8.38 years) with a FAP of 24%. In Fig. 16(b), we also show the $\langle S \rangle$ phased with this period and the harmonic curve that best fits these points with a confidence level of 80%. The point for $\langle S \rangle \sim 0.16$, which significantly deviates from the harmonic curve, corresponds to the only registry of activity we have for the year 2000 and it is, therefore, not statistically representative of the mean annual activity.

Our results are consistent with the decline in X-ray luminosity after 2005 reported by Robrade et al. (2007).

HD 131156 A - ξ Boo

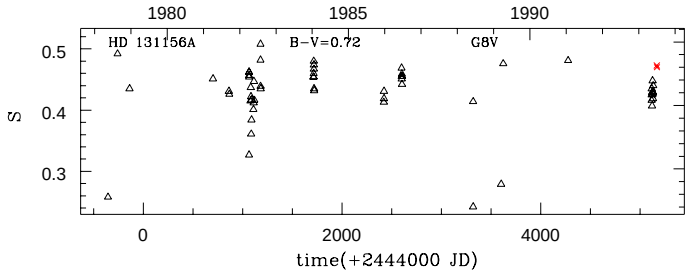

Fig. 17. Data for HD 131156A. Symbols as in Fig. 7.

HD 131156A is another flare star, which belongs to the visual binary system ξ Boo. It presented chromospheric variations of 55% during 1982 and of 90% during 1978. Baliunas et al. (1995) reported that HD 1311156A is a variable star without any evident cyclic behaviour. We analysed the mean annual $\langle S \rangle$ of the data plotted in Fig. 17 with the Lomb-Scargle periodogram, but we did not obtain a significant period. Baliunas et al. (1995) reported an $\langle S \rangle$=0.461 between 1966 to 1993 and we found an $\langle S \rangle$ 7% lower from 1978 to 1994 (Table 2). These values are similar within the standard deviation, a fact which supports our calibration.

5. Summary and Conclusions

The main purpose of this work is to incorporate the UV spectroscopic observations available in the IUE archives,

and, in particular, using the Mg II h and k lines, to the systematic studies of magnetic activity in solar-type stars. This allows us to extend the temporal span covered with these studies.

First, we analysed the ultraviolet continuum flux near the Mg II lines, and we obtained a relation between the mean UV continuum flux and the colour $B-V$ of the star. We also found that there is an activity component in this continuum flux. Therefore, an activity index constructed as the ratio of the fluxes in the Mg II line-cores and the continuum, similar to the Mount Wilson S-index, is not the best tool for the analysis of chromospheric activity, since part of the activity-related signal cancels out.

Subsequently, we analysed the relation between the Mount Wilson index and the Mg II line-core fluxes for a set of 117 nearly simultaneous observations of Mg II and Ca II fluxes of 21 F5 to K3 main sequence stars. We obtained that the relation between the Mount Wilson S-index and the Mg II fluxes depends on the stellar colour (i.e. spectral type), and we found the relation between the index S and the Mg II line-core flux and the stars's $B-V$.

From this calibration, we computed the Mount Wilson $S-$index for all high resolution IUE spectra of F, G and K main sequence stars, totaling 1623 spectra of 259 stars.

To study the evolution of activity levels for the most observed stars, we used these indices together with the Mount Wilson indices derived from several spectra in the visible wavelength range, obtained at CTIO (Henry et al., 1996) and at CASLEO (Cincunegui et al., 2007). In this way the data cover the period between 1978 and 2005.

For the most frequently observed stars of this sample, we analysed the level of activity over decades of time and also studied the short-scale variations. In particular, we analysed the data of each star with the Lomb-Scargle periodogram searching for periodic patterns analogous to the solar cycle. We confirmed that HD 22049 (ϵ Eri, K2V) and HD 2151 (β Hydri, G2IV) present chromospheric activity cycles of $\sim$5 and $\sim$12 years, respectively. We also found evidence of an activity cycle for HD 128621 (α Cen B, K1V), with a period of $\sim$8 years, which, to our knowledge, has not been reported in the literature. In particular, from our registry of activity, we obtained a rotation period of $\sim$35 days for HD 128621, similar to the one reported by Jay et al. (1997). On the other hand, we did not find a cyclic pattern in the periodogram of its companion HD 128620 (α Cen A, G2V).

References

Baliunas, S. L., Donahue, R. A., Soon, W. H., et al. 1995, ApJ, 438, 269
Boehm-Vitense, E. 1981, ARA&A, 19, 295
Brickhouse, N. S. & Dupree, A. K. 1998, ApJ, 502, 918
Cassatella, A., Altamore, A., González-Riestra, R., et al. 2000, Astron. Astrophys. Suppl. Ser., 141, 331
Cerruti-Sola, M., Cheng, C.-C., & Pallavicini, R. 1992, A&A, 256, 185
Cincunegui, C., Díaz, R. F., & Mauas, P. J. D. 2007, A&A, 469, 309
Donahue, R. A., Saar, S. H., & Baliunas, S. L. 1996, ApJ, 466, 384
Dravins, D., Linde, P., Fredga, K., & Gahm, G. F. 1993, ApJ, 403, 396
Dravins, D., Lindegren, L., & Vandenberg, D. A. 1998, A&A, 330, 1077
Fernandes, J., Lebreton, Y., Baglin, A., & Morel, P. 1998, A&A, 338, 455
Flower, P. J. 1996, ApJ, 469, 355
Frodesen, G. A., Skjeggestad, O., & Tofte, H. 1979, Probability and Statistics in Particle Physics (Universitetsforlaget)
Garhart, M. P., Smith, M. A., Turnrose, B. E., Levay, K. L., & Thompson, R. W. 1997, IUE NASA Newsletter, 57, 1
Gray, D. F. & Baliunas, S. L. 1994, ApJ, 427, 1042
Gray, D. F. & Baliunas, S. L. 1995, ApJ, 441, 436
Guedel, M., Guinan, E. F., & Skinner, S. L. 1997, ApJ, 483, 947
Guenther, D. B. & Demarque, P. 2000, ApJ, 531, 503
Hall, J. C., Lockwood, G. W., & Skiff, B. A. 2007, AJ, 133, 862
Hallam, K. L., Altner, B., & Endal, A. S. 1991, ApJ, 372, 610
Heath, D. F. & Schlesinger, B. M. 1986, J. Geophys. Res., 91, 8672
Henry, T. J., Soderblom, D. R., Donahue, R. A., & Baliunas, S. L. 1996, AJ, 111, 439
Hoeg, E., Bässgen, G., Bastian, U., et al. 1997, A&A, 323, L57
Horne, J. H. & Baliunas, S. L. 1986, ApJ, 302, 757
Jay, J. E., Guinan, E. F., Morgan, N. D., Messina, S., & Jassour, D. 1997, in Bulletin of the American Astronomical Society, Vol. 29, Bulletin of the American Astronomical Society, 730
Judge, P. G., Saar, S. H., Carlsson, M., & Ayres, T. R. 2004, ApJ, 609, 392
Kamper, K. W. & Wesselink, A. J. 1978, AJ, 83, 1653
Lachaume, R., Dominik, C., Lanz, T., & Habing, H. J. 1999, A&A, 348, 897
Messina, S. & Guinan, E. F. 2002, A&A, 393, 225
Metcalfe, T. S., Dziembowski, W. A., Judge, P. G., & Snow, M. 2007, MNRAS, L50+
Nordström, B., Mayor, M., Andersen, J., et al. 2004, A&A, 418, 989
Oranje, B. J. & Zwaan, C. 1985, A&A, 147, 265
Oranje, B. J., Zwaan, C., & Middelkoop, F. 1982, A&A, 110, 30
Perryman, M. A. C., Lindegren, L., Kovalevsky, J., et al. 1997, A&A, 323, L49
Press, W. H., Teukolsky, S. A., Vetterling, W. T., & Flannery, B. P. 1992, Numerical recipes in FORTRAN. The art of scientific computing (Cambridge: University Press, —c1992, 2nd ed.)
Robrade, J., Schmitt, J. H. M. M., & Favata, F. 2005, A&A, 442, 315
Robrade, J., Schmitt, J. H. M. M., & Hempelmann, A. 2007, Memorie della Societa Astronomica Italiana, 78, 311
Rutten, R. G. M. 1984, A&A, 130, 353
Rutten, R. G. M., Schrijver, C. J., Lemmens, A. F. P., & Zwaan, C. 1991, A&A, 252, 203
Saar, S. H. & Osten, R. A. 1997, MNRAS, 284, 803
Saffe, C., Gómez, M., & Chavero, C. 2005, A&A, 443, 609
Scargle, J. D. 1982, ApJ, 263, 835
Schmitt, J. H. M. M. & Liefke, C. 2004, A&A, 417, 651
Schrijver, C. J. 1987, A&A, 172, 111
Schrijver, C. J., Dobson, A. K., & Radick, R. R. 1989, ApJ, 341, 1035
Schrijver, C. J., Dobson, A. K., & Radick, R. R. 1992, A&A, 258, 432

Table 2. Long and short term variability records of the stars most observed by IUE.

Star HD	Sp. type & class	$B-V$	P_{rot}[d] (days)	Approx.[c] age (Gyr)	Mean activity $\langle S \rangle$[e]	Long scale[a] variability ($\sim$ decades) S_{min}/S_{max}	Period of time	Short scale[b] variability ($\sim$ month) S_{min}/S_{max}	Year
1835	G3V	0.67	7.78 [a]	0.6 [1]	0.334	0.315/0.353	1981-2005	0.307/0.355	1991
2151	G2IV	0.62	28.00 [b]	6.7 [2]	0.153	0.133/0.163	1978-1995	0.160/0.183	1985
								0.141/0.171	1993
								0.145/0.164	1994
10700	G8V	0.72	34.50 [c]	7.2 [3]	0.175	0.171/0.186	1983-2004	0.167/0.173	1993
								0.172/0.178	2002
								0.172/0.181	2003
								0.169/0.179	2004
20630	G5V	0.68	9.24 [a]	0.7 [1]	0.370	0.334/0.419	1980-1994	0.357/0.382	1985
								0.318/0.364	1994
22049	K2V	0.88	11.68 [a]	0.7/0.9 [4]	0.473	0.426/0.520	1978-2005	0.449/0.504	1980
								0.395/0.460	1982
								0.495/0.519	1983
								0.422/0.475	1986
								0.423/0.459	2002
								0.450/0.569	2003
39587	G0V	0.59	5.89 [a]	5.6 [5]	0.335	0.180/0.375	1978-1993	0.327/0.358	1984
115383	G0V	0.59	3.33 [a]	5.1 [5]	0.332	0.248/0.362	1978-1995	0.296/0.375	1993
128620	G2V	0.71	29.00 [d]	6.8/7.6 [7]	0.167	0.153/0.185	1978-2004	0.133/0.192	1995
128621	K1V	0.88	36.90 [e]	6.8/7.6 [7]	0.214	0.162/0.248	1978-2004	0.216/0.247	1978
								0.192/0.230	1980
								0.167/0.229	1982
								0.206/0.225	1983
								0.169/0.297	1995
131156	G8V	0.76	6.31 [a]	2 [8]	0.430	0.242/0.508	1978-1993	0.258/0.492	1978
								0.327/0.508	1982
								0.413/0.431	1985
								0.442/0.469	1986
								0.407/0.473	1993
133640	G0Vnvar	0.65	0.28 [f]	15.4 [5]	0.272	0.263/0.276	1978-1990	0.241/0.307	1979
								0.256/0.297	1989

[a] Maximum and minimum level of activity reached along decades.

[b] Variations recorded in particular years.

[c] References for age: 1. Messina & Guinan (2002), 2. Dravins et al. (1998), 3. Lachaume et al. (1999), 4. Saffe et al. (2005), 5. Nordström et al. (2004) , 7. Guenther & Demarque (2000) and 8. Fernandes et al. (1998).

[d] References for P_{rot}: a. Donahue et al. (1996), b. Guedel et al. (1997) , c. Saar & Osten (1997), d. Hallam et al. (1991), e. Jay et al. (1997) and f. Brickhouse & Dupree (1998).

[e] Mean annual Mount Wilson index.

Table 3. Index S derived from all the high resolution spectra of F, G and K dwarf stars observed by IUE.

[a] HD	m_V	$B-V$	Plx(mas)	Julian date[b]	Year[a]	S[c]	σ_S[d]	IUE spectrum
166	6.07	0.752	72.98	2445182.000	1982.58	0.404	0.0161	LWR13815
166	6.07	0.752	72.98	2445290.000	1982.87	0.467	0.0189	LWR14642
166	6.07	0.752	72.98	2445291.000	1982.87	0.447	0.0180	LWR14654
166	6.07	0.752	72.98	2445292.500	1982.87	0.451	0.0182	LWR14663
400	6.21	0.504	30.26	2445998.500	1984.81	0.156	0.0058	LWP04632
432	2.28	0.380	59.89	2444521.250	1980.76	0.159	0.0059	LWR08974
432	2.28	0.380	59.89	2447112.000	1987.85	0.157	0.0058	LWP12076
432	2.28	0.380	59.89	2444509.000	1980.73	0.159	0.0058	LWR08895
432	2.28	0.380	59.89	2447111.750	1987.85	0.161	0.0059	LWP12074
432	2.28	0.380	59.89	2447111.750	1987.85	0.159	0.0059	LWP12068
432	2.28	0.380	59.89	2447111.500	1987.85	0.161	0.0059	LWP12067
432	2.28	0.380	59.89	2447027.000	1987.63	0.160	0.0059	LWP11431
432	2.28	0.380	59.89	2447111.750	1987.85	0.165	0.0061	LWP12070
432	2.28	0.380	59.89	2444085.250	1979.58	0.138	0.0052	LWR05214
432	2.28	0.380	59.89	2446676.750	1986.67	0.163	0.0060	LWP08997
432	2.28	0.380	59.89	2446676.750	1986.67	0.161	0.0059	LWP08996
432	2.28	0.380	59.89	2447111.750	1987.85	0.162	0.0059	LWP12073
432	2.28	0.380	59.89	2447112.000	1987.85	0.164	0.0060	LWP12075
432	2.28	0.380	59.89	2447111.750	1987.85	0.165	0.0061	LWP12071
432	2.28	0.380	59.89	2447111.750	1987.85	0.164	0.0060	LWP12069
432	2.28	0.380	59.89	2447111.750	1987.85	0.163	0.0060	LWP12072
432	2.28	0.380	59.89	2446677.000	1986.67	0.164	0.0060	LWP08999
432	2.28	0.380	59.89	2446677.000	1986.67	0.163	0.0060	LWP09000
432	2.28	0.380	59.89	2446677.000	1986.67	0.167	0.0061	LWP08998
432	2.28	0.380	59.89	2446677.000	1986.67	0.168	0.0062	LWP09001
483	7.07	0.644	19.28	2447899.000	1990.02	0.276	0.0105	LWP17097
693	4.89	0.487	52.94	2445641.750	1983.83	0.136	0.0051	LWP02201
905	5.71	0.331	28.57	2444523.500	1980.77	0.173	0.0063	LWR08992
1581	4.23	0.576	116.38	2444748.250	1981.39	0.139	0.0052	LWR10687
1581	4.23	0.576	116.38	2444729.500	1981.34	0.138	0.0052	LWR10520
1581	4.23	0.576	116.38	2444770.500	1981.45	0.139	0.0052	LWR10858
1581	4.23	0.576	116.38	2445059.750	1982.25	0.146	0.0054	LWR12915
1581	4.23	0.576	116.38	2443710.500	1978.55	0.127	0.0049	LWR01862
1581	4.23	0.576	116.38	2443798.000	1978.78	0.126	0.0049	LWR02621
1581	4.23	0.576	116.38	2444762.500	1981.43	0.146	0.0054	LWR10799
1581	4.23	0.576	116.38	2443912.000	1979.10	0.152	0.0056	LWR03699
1581	4.23	0.576	116.38	2446038.000	1984.91	0.153	0.0057	LWP04914
1581	4.23	0.576	116.38	2443748.500	1978.65	0.136	0.0051	LWR02191

[a] The full table is available in electronic form at the CDS via http://cdsweb.u-strasbg.fr/cgi-bin/qcat?J/A+A/ .
[b] IUE spectrum date.
[c] Mount Wilson Index derived from IUE spectrum.
[d] Mount Wilson Index standard deviation